Semi-Annual Technical Report

1 July 1971 - 1 January 1972

NEW METHODS FOR GROWTH AND CHARACTERIZATION OF GaAs AND MIXED III-V SEMICONDUCTOR CRYSTALS

University of Southern California
Los Angeles, California 90007

Submitted to

ADVANCED RESEARCH PROJECTS AGENCY

ARPA Order Number 1623
Grant Number DAHC15-71-G6
1 July 1971 - 30 June 1971
$184,586.00

Principal Investigator: William R. Wilcox
(213) 746-6203

The views and conclusions contained in this document are those of the authors and should not be interpreted as necessarily representing the official policies, either expressed or implied, of the Advanced Research Projects Agency or the U.S. Government.

SUMMARY

The purpose of this program is to develop new and improved methods for the growth and characterization of gallium arsenide (GaAs) and mixed III-V semiconductor crystals. This is being accomplished by laboratory experiments and related theoretical research. The program is a continuation of one initiated in July 1970 under ARPA Order Number 1628, Grant Number DAHC15-70-G14.

A new Czochralski technique has been developed which permits fairly routine growth of dislocation-free GaAs crystals. An apparatus for liquid-encapsulated floating-zone melting of III-V crystals has been constructed and is gradually being debugged. The kinetics of drying and moisture absorption by boron oxide encapsulant have been measured and published. Further improvements have been made in the travelling heater growth method. Studies on an organic analog system have elucidated the conditions required for good single crystal growth by the travelling heater method. A new method is being developed to lower oxygen concentrations during liquid epitaxial growth of GaAs, so as to permit growth at significantly lower temperatures. It has been found that stirring (e.g., by rotation) substantially reduces incorporation of solid foreign particles into a growing crystal. Volatile solvent inclusions were observed to boil when the temperature is sufficiently high in a crystal. This boiling altered the migration rates and directions when a temperature gradient was simultaneously applied.

The influence of bending and short term heating on mobility and carrier concentration of GaAs has been studied. The mobility of our crystals generally decreased as the carrier concentration increased. The high-impedance Hall apparatus appears to be nearly complete. Further

theoretical developments have led to improved understanding of photoemission from Schottky barriers. Photoluminescence measurements confirmed that our Czochralski-grown crystals are less pure than our horizontal Bridgman-grown crystals.

Six scientific papers have resulted from this program in the last six months.

The following equipment was purchased under this grant and is now installed in our laboratories: ellipsometer, Cat to TTY interface, gas laser and power supply, polisher, high voltage power supply, temperature controller, power assembly for X-ray generator, volt-ohmmeter and sodium vapor lamp.

RESPONSIBLE STAFF

Staff	Responsibility	Sections in Report
W. R. Wilcox	Program coordination, crystal growth research.	I.C,D,F.
W. P. Allred	Liquid-seal Czochralski technique.	I.A.
E. S. Johnson	Liquid-encapsulated floating-zone melting and luminescence measurements.	I.B, II.F.
J. M. Whelan	Liquid epitaxial growth.	I.E.
A. L. Esquivel	Dislocation studies.	II.A.
D. B. Wittry	Electron microprobe studies.	II.B.
C. R. Crowell	Electronic properties.	II.C,D,E.

CONTENTS

	Page
SUMMARY	ii
RESPONSIBLE STAFF	iv
I. CRYSTAL GROWTH	1
A. Liquid-Seal Czochralski Technique	1
B. Liquid-Encapsulated Floating-Zone Melting	2
C. Drying of Boron Oxide	3
D. Travelling Heater Method	3
E. Oxygen Removal Rates from Liquid Phase GaAs Epitaxial Systems	16
F. Related Crystal Growth Research	20
II. CHARACTERIZATION	26
A. Dislocation Studies and Electrical Properties	26
B. Cathodoluminescence and Stimulated Emission Studies	37
C. High Impedance Hall Apparatus	39
D. Tunnel and Thermal Effects in Photoemission from Schottky Barriers	39
E. Schottky Barrier-Capacitance Characterization of Impurities	40
F. GaAs Photoluminescence Measurements	42
REFERENCES	45

I. CRYSTAL GROWTH

A. Liquid-Seal Czochralski Technique

As reported previously [1], we have invented a new Czochralski technique for GaAs which utilizes a pull rod sealed by molten B_2O_3. (The B_2O_3 is not in contact with the surface of the GaAs melt.) We are now able to grow dislocation-free single crystals of GaAs by this technique. We have not yet been able to grow high-purity uncompensated crystals, however. Our undoped crystals have a resistivity of about 10^8 ohm cm. Crystals doped with tellurium to about $10^{15}/cm^3$ have low mobilities compared with crystals grown by the horizontal Bridgman method. This indicates the presence of a deep-level impurity. Mass spectrographic analysis (courtesy of the Air Force Cambridge Research Laboratory) has been performed on one of these crystals. Al, Si and Cl were found, but no Cu. Infrared absorption measurements at USC (courtesy of Prof. Spitzer) failed to reveal the presence of Si, however, Thus the identify of the recombination center(s) remains a mystery.

Two sources of contamination have been considered - the B_2O_3 and the vitreous carbon crucible. High purity B_2O_3 was recently used in growing several crystals, with no improvement in crystal purity observed. Therefore other crucible materials are being considered as a replacement for the vitreous carbon. Fused silica is undesirable because of likely contamination of the crystals with silicon. Aluminum oxide is good from a purity standpoint, but presents other problems. With radio-frequency induction heating, either a susceptor must be placed around the alumina crucible or the power must be coupled directly to the GaAs. We do not believe such direct coupling will produce the thermal conditions required for growth of dislocation-free crystals. Nevertheless this has been tried. These

attempts failed because the alumina crucibles fractured due to thermal stresses.

At the moment we are considering the use of silicon as a crucible material. The silicon would be coated, e.g., with boron nitride and/or pyrolytic graphite, to prevent attack of the crucible by the melt and contamination of the crystal by silicon. Pyrolytic graphite crucibles are another possibility being explored.

These crystals are being characterized by the methods described in Section II of this report. We also plan to supply crystals to device fabricators for testing in devices. An arrangement for obtaining mass spectrographic analyses is being negotiated with Battelle Memorial Institute.

B. Liquid-Encapsulated Floating-Zone Melting

We have completed construction of the previously described [1] apparatus for float zoning of GaAs while surrounded by a molten encapsulant to prevent As evaporation. Several tests have been performed using B_2O_3 as the encapsulant. A molten GaAs zone has been held within the encapsulant and other basic features of the apparatus appear to be sound. However, excessive rf coupling to the control electronics and arcing to the supplementary heaters necessitated extensive rebuilding of the control systems. Previous difficulties now appear to be corrected. The rebuilt apparatus is shown in operation in Figure 1. Further attempts to move the molten zone and obtain floating-zone purification and crystallization will be made in the near future. Presently, feed rods are being prepared as described in detail in Section I.D. Growth of mixed III-V materials will eventually be attempted. We will also attempt to find higher density encapsulants so as to enable growth of larger diameter crystals.

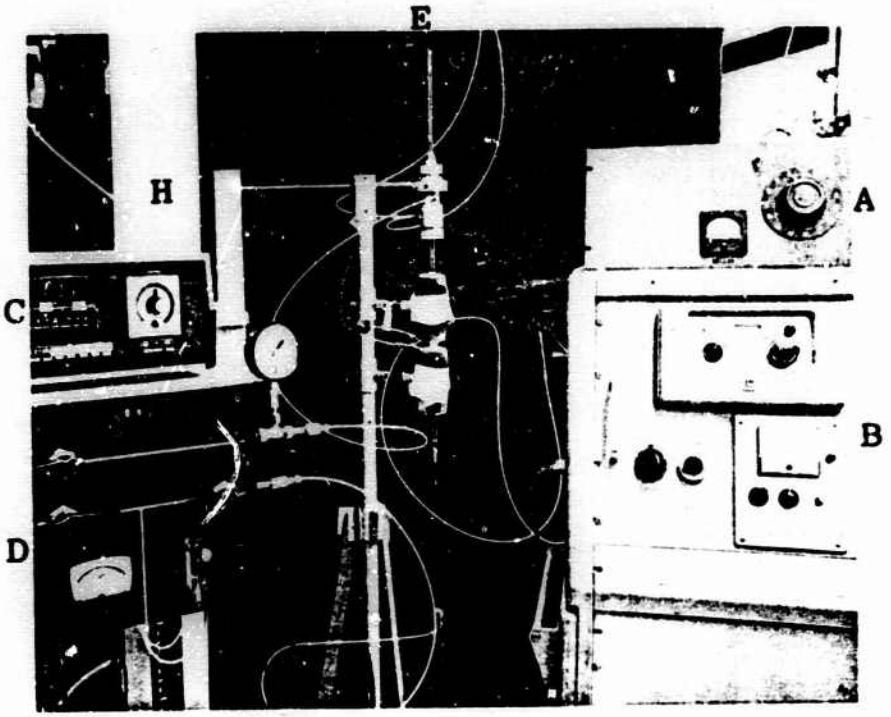

Figure 1. Photographs of the Liquid-Encapsulated Floating-Zone Melting Apparatus for Growth of High Purity GaAs and Mixed III-V Crystals.

A. Control for auxiliary heaters (G).

B. Controls for radio-frequency generator (J).

C. Controls for controlled-motion table (H).

D. Vacuum system.

E. Zone melting tube and chuck assembly.

F. Induction coil and molten zone.

G. Auxiliary heaters to keep B_2O_3 molten.

H. Controller motion table.

I. Standard clamps for heaters.

J. Radio-frequency generator.

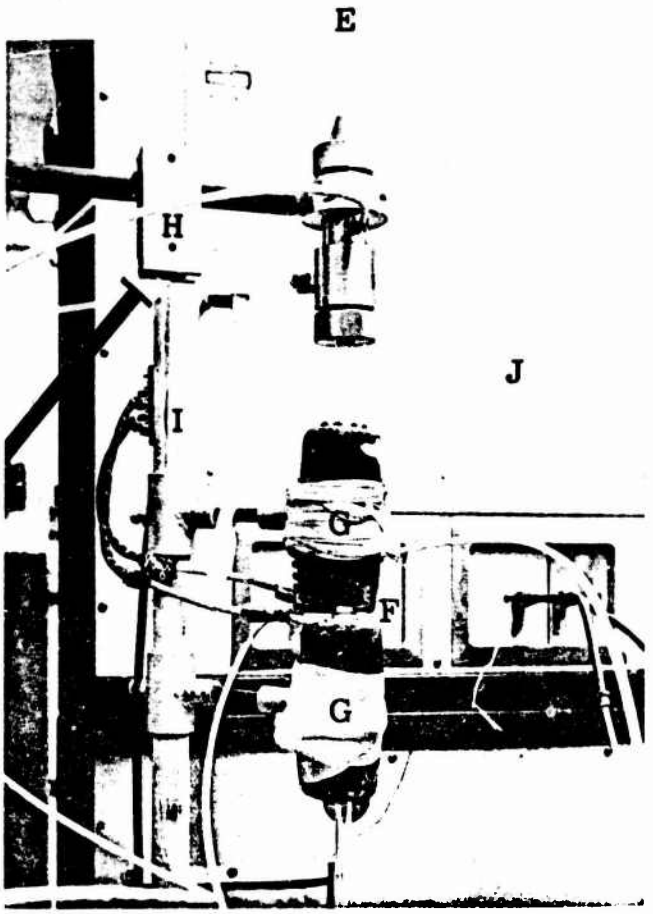

Close-up.

C. Drying of Boron Oxide

The experiments on drying of B_2O_3 encapsulant have been completed and a paper published [2]. Figure 2 shows the exponential decrease in water content during bubbling of dry nitrogen through molten B_2O_3 at 1200°C, as monitored by infrared absorption measurements. The upper curve is for thin samples while the bottom curve is for thick samples, indicating that some moisture was reabsorbed from the air during sampling. Figure 3 shows moisture absorption when vitreous B_2O_3 was exposed to air at room temperature. The first region is parabolic, corresponding to diffusion limited absorption. The surface was smooth during this period. The second region is linear - a constant absorption rate. The B_2O_3 surface was powdery during this period and gave an X-ray powder pattern for boric acid. Figure 4 shows removal of surface moisture from B_2O_3 by exposure to a vacuum at room temperature. The curve is a sum of two exponentials, indicating two parallel removal mechanisms - probably involving boric acid conversion to B_2O_3 and water diffusion and desorption from B_2O_3.

D. Travelling Heater Method

As reported previously [1], we have grown bulk GaAs single crystals by the travelling heater method. In order to permit systematic studies of the influence of the growh parameters, the growth procedure is being improved. Endeavors are centered on improving the temperature control, the heater lifetime, the preparation of feed and seed crystals, and the loading procedure for the growth ampoule.

A Sola constant voltage transformer combined with a variable autotransformer was found to provide a constant power input ideal for the long growth period required (~one week). Heaters are now made by winding 22 gauge platinum wire on grooved alundum tubes. This will permit heater

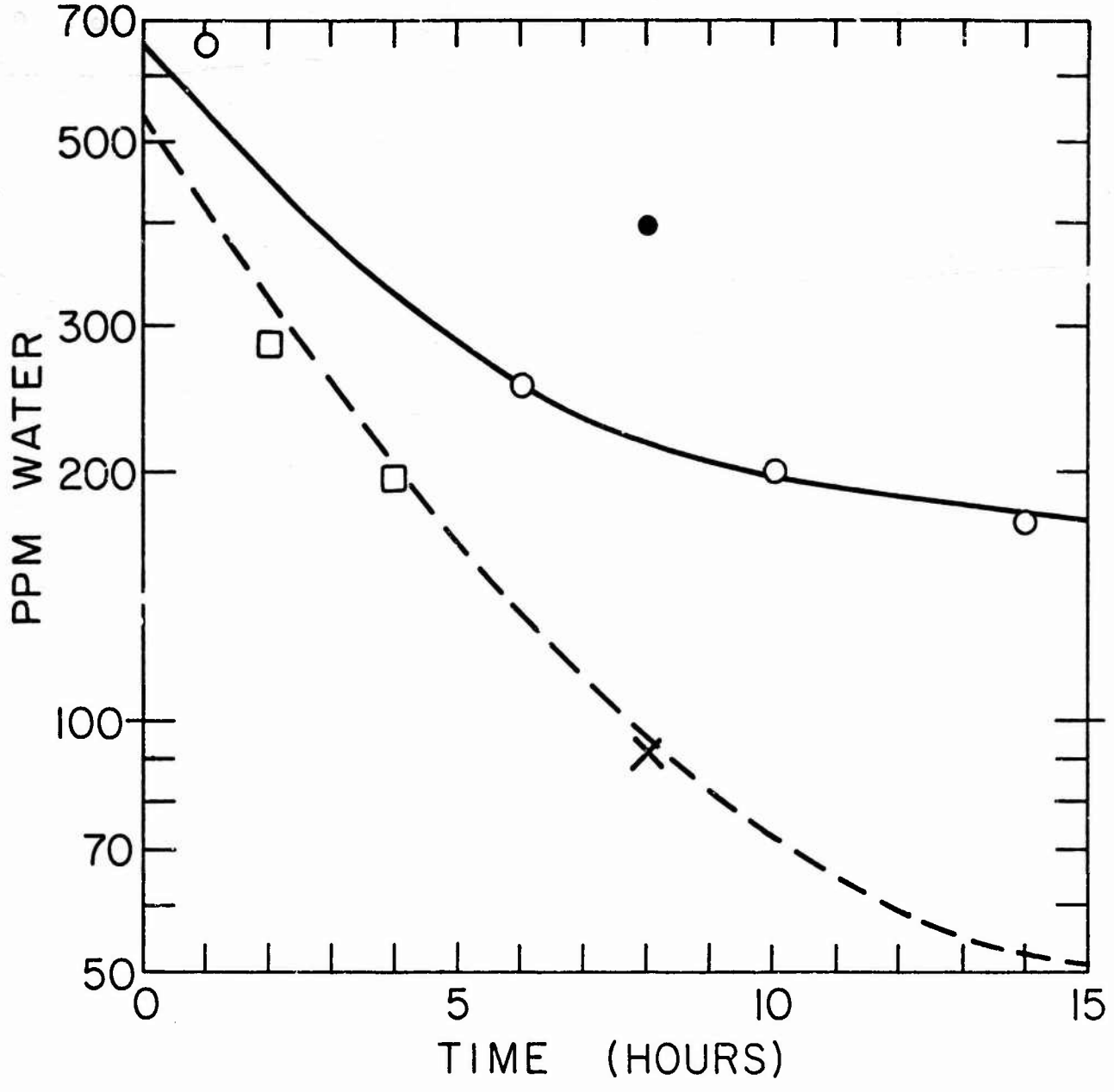

Figure 2. Rate of Removal of Water from Molten B_2O_3 by Bubbling Dry Nitrogen at 1200°C.

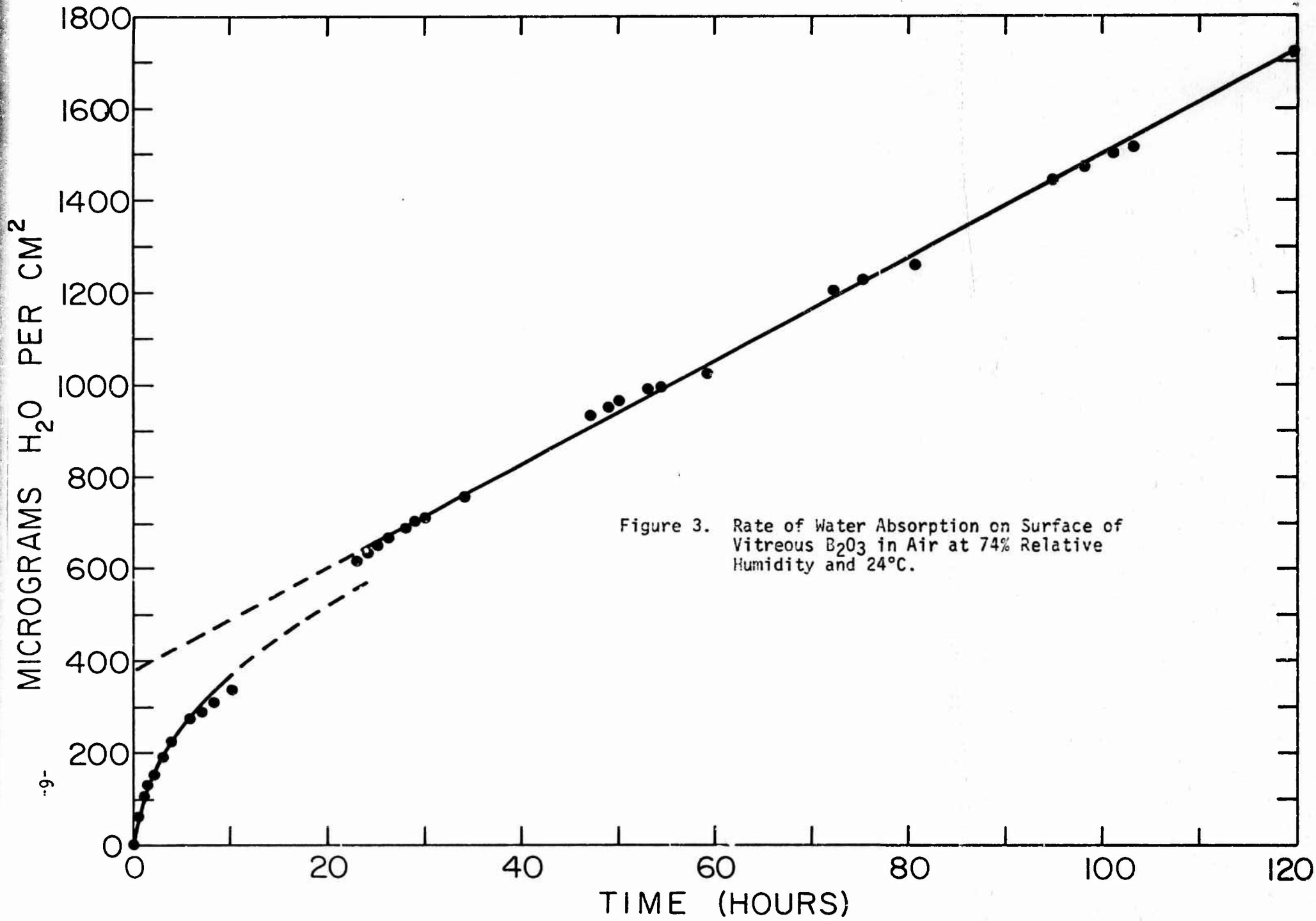

Figure 3. Rate of Water Absorption on Surface of Vitreous B_2O_3 in Air at 74% Relative Humidity and 24°C.

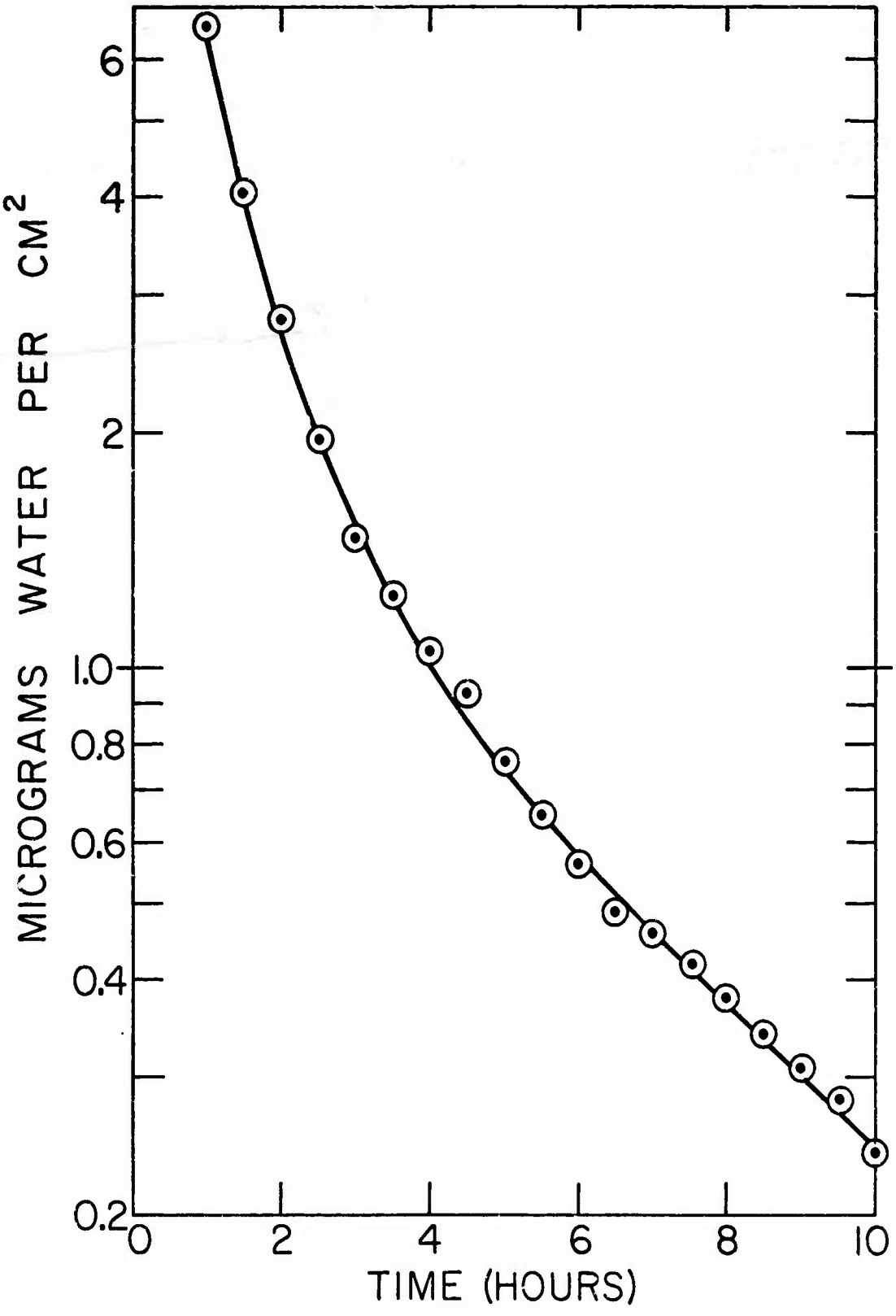

Figure 4. Rate of Removal of Surface Moisture in Vacuum at 24°C.

temperatures up to ~1200°C without a high risk of failure during growth.

For the travelling heater method, the feed material must fit snugly in the growth ampoule. Previously we had prepared cylindrical feed rods by grinding horizontal-Bridgman GaAs crystals of semi-circular cross section - a wasteful and time-consuming procedure. We have found that GaAs can be cast into cylindrical rods. Pieces of GaAs were loaded into a fused silica tube of the same diameter as the growth ampoule. This was in turn inserted into a larger diameter silica tube which was evacuated and sealed. This ampoule was placed inside a resistance furnace. The temperature was raised to 1250 to 1260°C and held for one to two hours to permit the GaAs to melt and settle. The temperature was then lowered at about 4°C/minute to room temperature by manually lowering the power input to the furnace. Although the inner tube cracked because of thermal stress, the resulting GaAs ingots were free of voids, pits or excessive cracks, as shown in Figure 5.

In an effort to further our understanding of the travelling heater method of growing III-V crystals, we are performing experiments with an organic analog. The analog system, naphthalene-benzoic acid, is transparent and melts below 120°C, which permits easy microscopic observation. Thus, for example, we can observe growth of individual grains with a smooth interface and breakdown of the interface with trapping of solvent, as shown in Figure 6. Initially, experiments were performed with the tube exposed to air. Drafts and variations in room temperature caused sufficient problems that an improved apparatus was necessary. A diagram of this improved apparatus is shown in Figure 7. Controlled temperature coolant was circulated through the top and bottom chambers. The electrical resistance heater was enclosed to avoid drafts. Fine thermocouples permitted measurement of temperatures at the heater, on the surface of the tube and inside the tube.

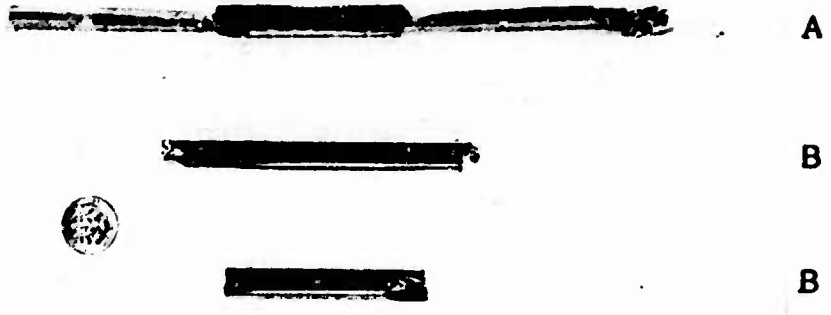

Figure 5. Photograph of Cast Ingots.

A. Assembled ampoule before melting.

B. Cast ingots.

Figure 6. Photographs of the Growing Interface of Naphthalene with Benzoic Acid Solvent. (The dark bands are the heater wire) x 15

Tube diameter: 10.6 mm

Length of zone: ~10 mm

Solvent Concentration: ~25 wt.%

Temperature gradient: ~39°C/cm.

A. Smooth interface showing grain boundaries.

Travel rate: 10.2 mm/day

B. Interface after breakdown showing trapping of solvent.

Travel rate: 26.3 mm/day

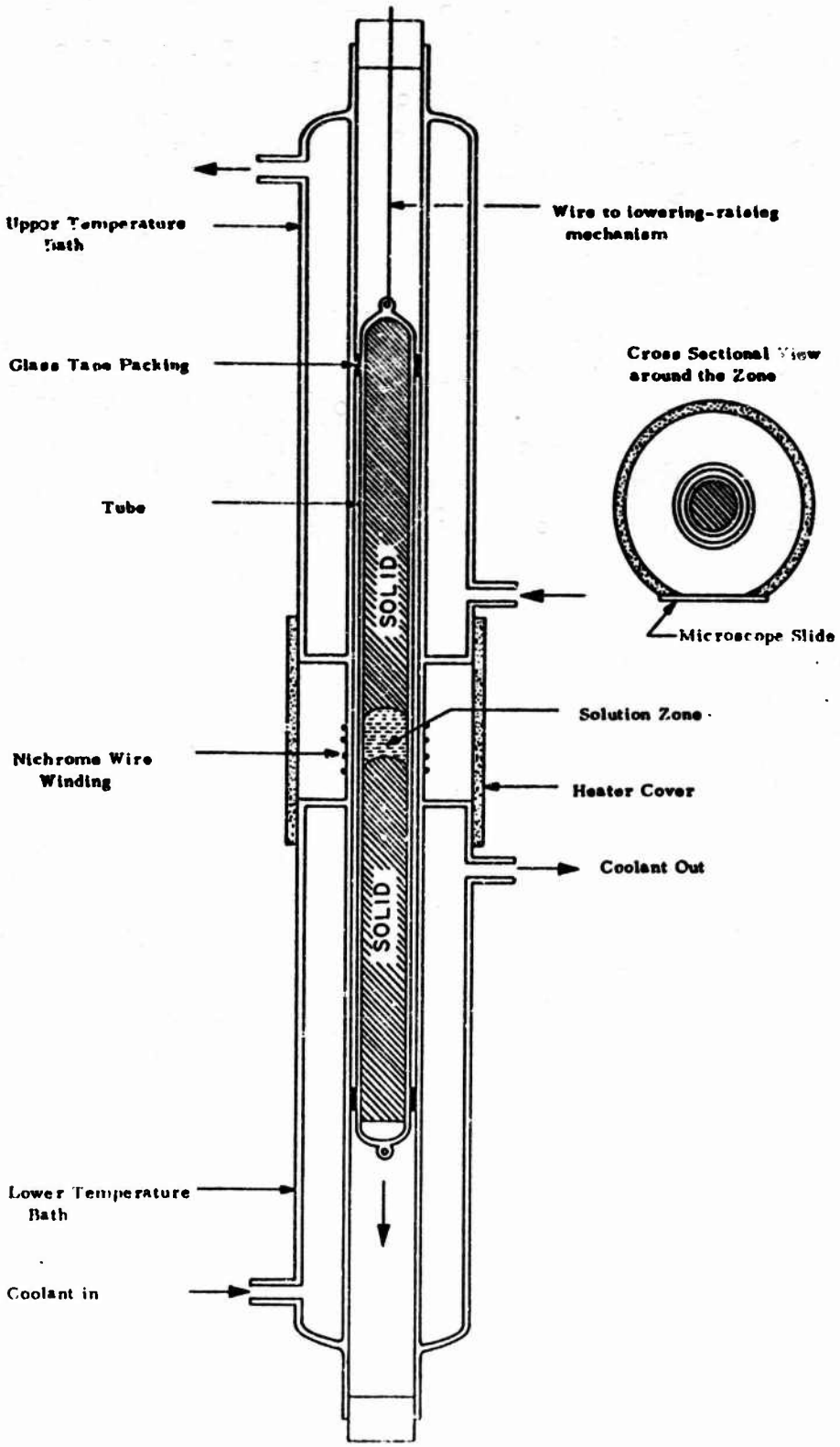

Figure 7. Schematic Drawing of Travelling Heater Apparatus Using Organic Analog to Semiconductor System. Tube extends farther than shown and is sealed at both ends to avoid a chimney effect.

By slowly lowering the tube containing a thermocouple through the heater, temperature profiles were obtained, as exemplified by Figure 8. The zone was displaced upward from the heater because of free convection both in the air space between the heater and the sample tube and in the solvent zone itself. Note that the temperature profile is roughly symmetrical with respect to the zone. Within experimental error the temperature at the upper and lower interfaces are identical, as they should be for very low travel rates. At higher potentiometer sensitivities, temperature oscillations were observed in the solution zone, as shown in Figure 9. This was another manifestation of free convection in the zone. The temperature fluctuations were greatest near the top of the zone and depended on the tube diameter.

The dependence of interface positions on travel rate was determined, as exemplified by Figure 10. As expected the interfaces were shifted in the direction of travel both because of latent heat effects and because of changes in interface temperatures required to drive the interfacial kinetics and the mass transfer across the zone.

We are developing theoretical insight into the travelling heater method concurrently with the experimental program. There are two basic problems in obtaining good single crystals by the travelling heater method - solvent inclusions and polycrystallinity. Solvent inclusions should arise when constitutional supercooling occurs. Our experiments confirm this, i.e., there is a critical freezing rate for interface breakdown and trapping of solvent which increases as the solvent concentration decreases (temperature of the zone increases) and as the temperature gradient increases.

We feel that a convex interface should produce single crystals while

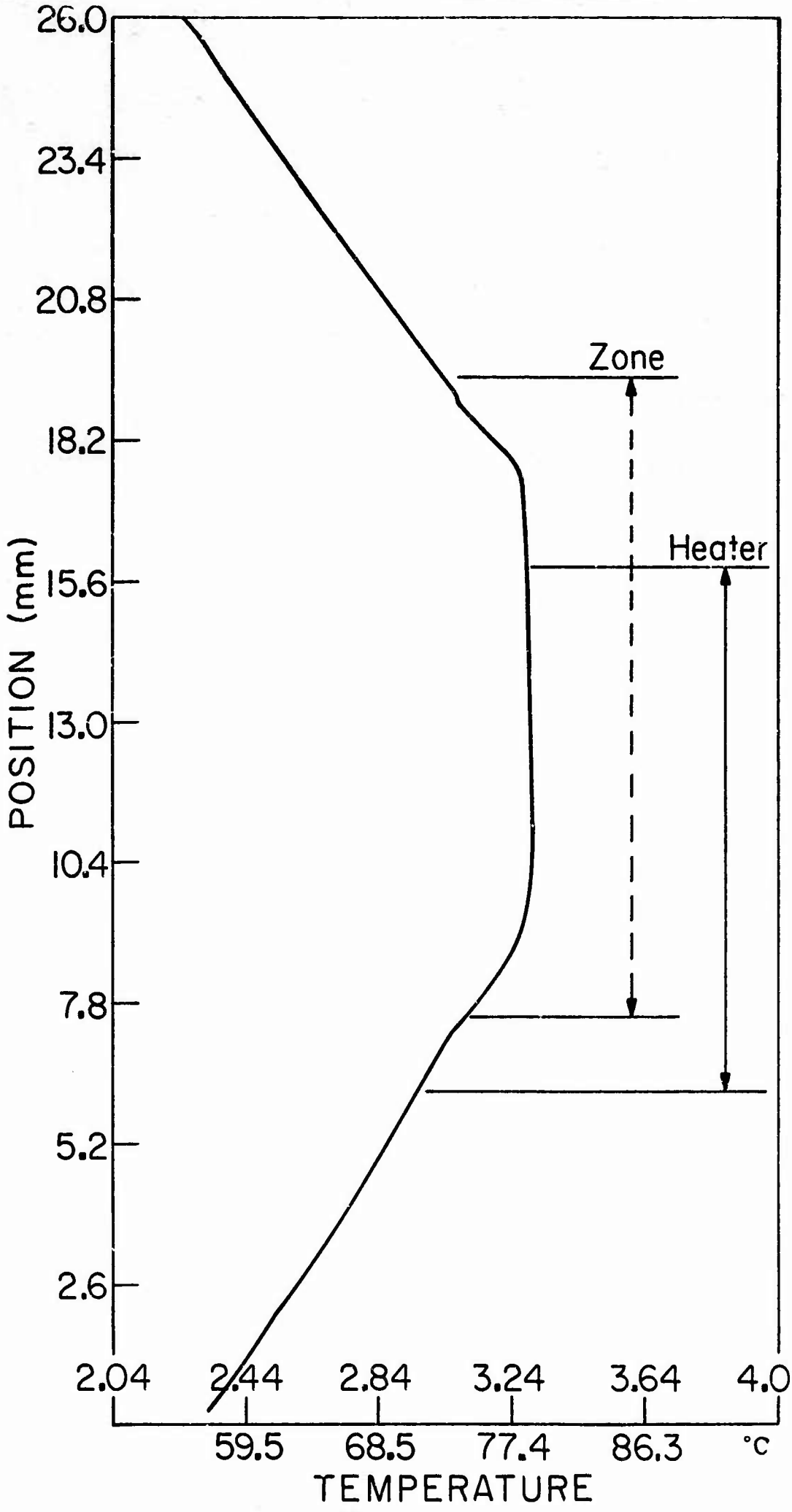

Figure 8. A typical Temperature Profile in the Organic Analog Travelling Heater Method Experiments.

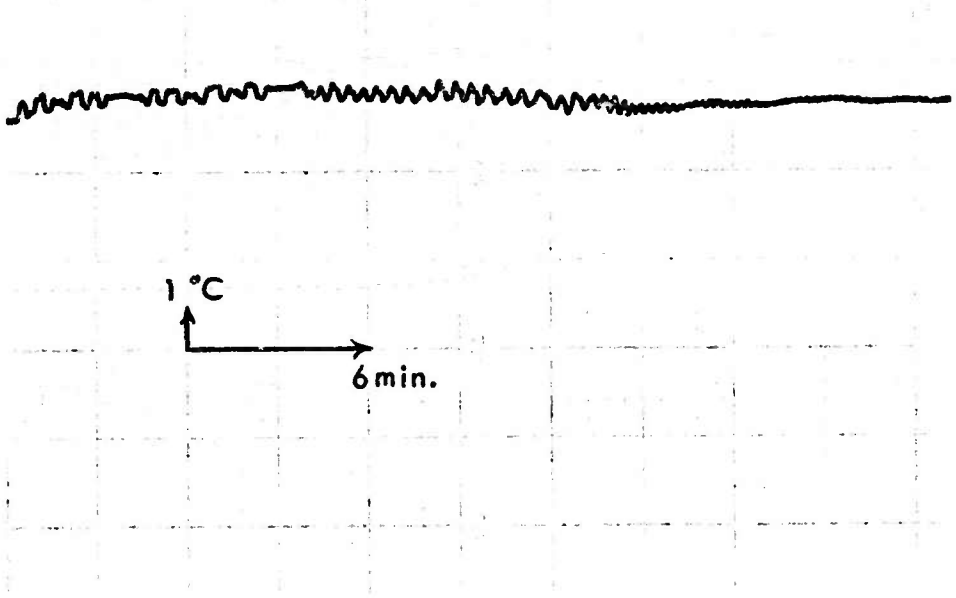

Figure 9. Typical Temperature Oscillations in the Benzoic Acid Solvent Zone.

Position: ~1.4 mm below top interface.

Travel Rate: 0.28 mm/hour (thermocouple moving with tube).

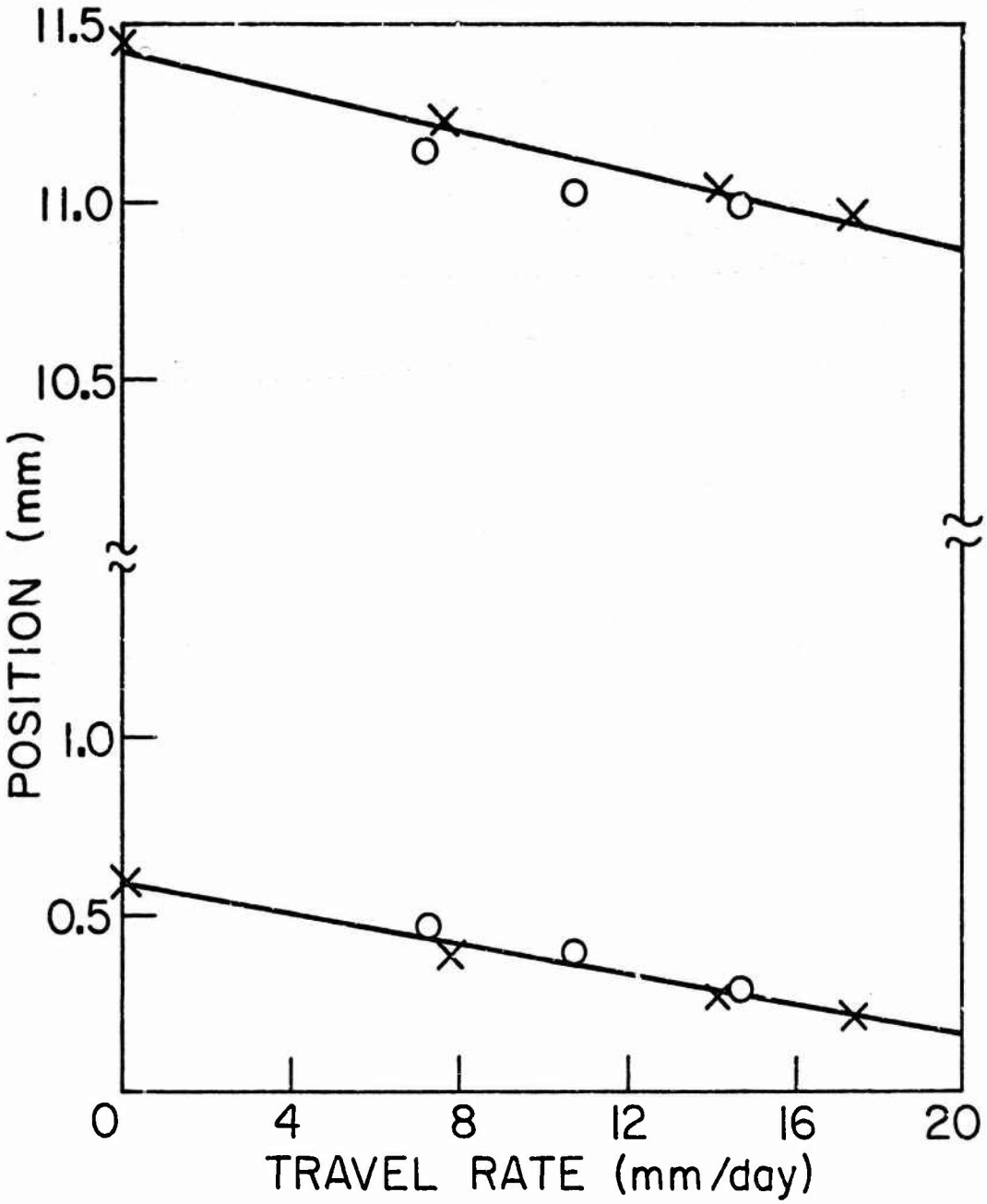

Figure 10. Interface Positions as a Function of Zone Travel Rate. Naphthalene-benzoic acid.

Tube diameter: 10.6 mm

Solvent concentration: 25 wt.%

Coolant bath temperature: 23°C

Temperature gradient: 39°C/cm

a concave interface should produce polycrystalline ingots because new grains nucleating at the tube walls will propagate to the center of the ingot. We have observed movement of grain boundaries on a convex interface to the outside to yield a single grain of naphthalene, as predicted. We feel that the interface will be convex when it lies within the heater and concave when it lies outside the heater. Our experiments confirm this. Theoretical calculations and quantitative experimental observations will be used together to place these bits of insight on a quantitative foundation.

E. Oxygen Removal Rates from Liquid Phase GaAs Epitaxial Systems

As reported previously [1], we are developing techniques to permit lower temperature growth of GaAs. The rates of oxygen removal from GaAs liquid phase epitaxial systems are dominant features which ultimately limit the minimum growth temperatures. Low growth temperatures are desirable in that the temperature control requirements for controlling film thicknesses are less, impurity solubilities are lower, and chemical reactivities are reduced.

The oxygen problem has two principal aspects. The first is oxygen chemiabsorbed on the seed, most likely as a GaAs-oxide more stable than $Ga_2O_3(s)$. In order to grow superior quality films it is necessary to remove this oxide prior to the growth. Manifestations of incomplete removal are irregular nucleation and the growth of films with poor surfaces.

Evidence for the presence of oxygen on the surface of GaAs substrates which were not reduced by H_2 in 30 minutes at 825°C was previously noted. The mole ratio of H_2O to H_2 in the exhaust gas line of a liquid phase epitaxial system was monitored by the emf of a ZrO_2-CaO cell operated at

700°K. The emf of this cell was stable to 1 mV and changed approximately 20 mV per decade change in the H_2O-H_2 mole ratio over its linear range. This was estimated to be the case for H_2O/H_2 ratios $\leq 10^{-6}$. For the reaction at 800°C the steady-state H_2O/H_2 ratio was $\sim 2 \times 10^{-6}$ with a H_2 flow rate of 100 cc/min. Without changing the flow conditions the emf of the ZrO_2 cell increased, indicating a lower H_2O/H_2 ratio when the reaction was cooled. This indicates that the reactor inlet H_2 was of higher quality and that it was degraded by the quartz reaction itself at 800°C. With the reaction at 800°C for several hours so that steady state conditions pertained, the seed was lowered into the furnace to a position just above the melt and so maintained for 30 minutes. At the end of this period the H_2O/H_2 ratio was at its original steady state value. Immersion of the seed in the Ga melt caused a momentary rise in H_2O/H_2 ratio. The Ga melt was slightly undersaturated. This rise indicates that the oxide on the substrate dissolved in the melt and the dissolved oxygen then reacted with the H_2 atmosphere to produce H_2O. Removal of the seed from the melt and subsequent immersion produced no detectable change in the exit H_2O/H_2 ratio. These experiences prompted the consideration of using an alternate method for removing oxygen from Ga melts.

One approach used in several laboratories elsewhere involves the use of carbon reactors contained in quartz. There are problems associated with adequately cleaning the carbon, avoiding reaction of carbon with the quartz and subsequent introduction of Si as an impurity. In principle, though, the carbon should be a good reducing agent for oxygen in Ga. H_2 is almost as good a reducing agent. The rates of removal are important. If one considers the dissolved oxygen in the Ga melt to be in equilibrium with the H_2 atmosphere (an optomistic assumption) and that the dissolved

oxygen removal rate is proportional to the partial pressure of H_2O (which we optomistically take as 10 ppm or 10^{-5} atm) and a reasonable H_2 flow rate of 100 cc atm min^{-1}, the removal rate of oxygen from the melt at 1000°K is

$$\text{moles of O removed from melt per minute} = \frac{10^{-5}\ \text{atm} \times 100\ \text{cc/min}}{1000\ \text{deg} \times 82\ \text{cc atm mol}^{-1}\text{deg}^{-1}} \simeq 10^{-8}\ \text{mol/min}$$

$$\simeq 1\ \text{monolayer/cm}^2\ \text{of substrate.}$$

This slow removal rate caused us to consider using electrolytic pumping to remove dissolved oxygen. Calcia-stabilized zirconia operating with an ion current of only 10 mA can remove oxygen at a rate of 3×10^{-6} moles/min or 300 times faster than a clean H_2 atmosphere. In addition, this pumping efficiency is to be anticipated for concentrations of oxygen below the saturation concentration at temperatures as low as 500°C.

The system designed to test this is shown in Figure 11. Its prime feature is the use of a calcia-stabilized zirconia pump which serves as the melt crucible. The other electrode (outside) is fired Pt paste operating in a H_2 atmosphere saturated with H_2O at 0°C to establish a known oxygen activity. A well designed Pd-Ag tube H_2 diffuser was graciously provided by Standard Telecommunications Laboratory. All valves are the improved West Glass Stopcocks with leak rates $\leq 4 \times 10^{-10}$ ssc atm sec^{-1}. The lengthy design time of this apparatus reflected the difficulties in preparing a flow system equivalent to a heated vacuum system required to produce a pressure of 10^{-4} atmosphere with a pumping speed of only 10^{-3} ℓ s^{-1}.

A feature included in the above apparatus is the provision for supplying an As partial pressure close to that in equilibrium with the GaAs seed. This was previously shown in this laboratory to be necessary if surface

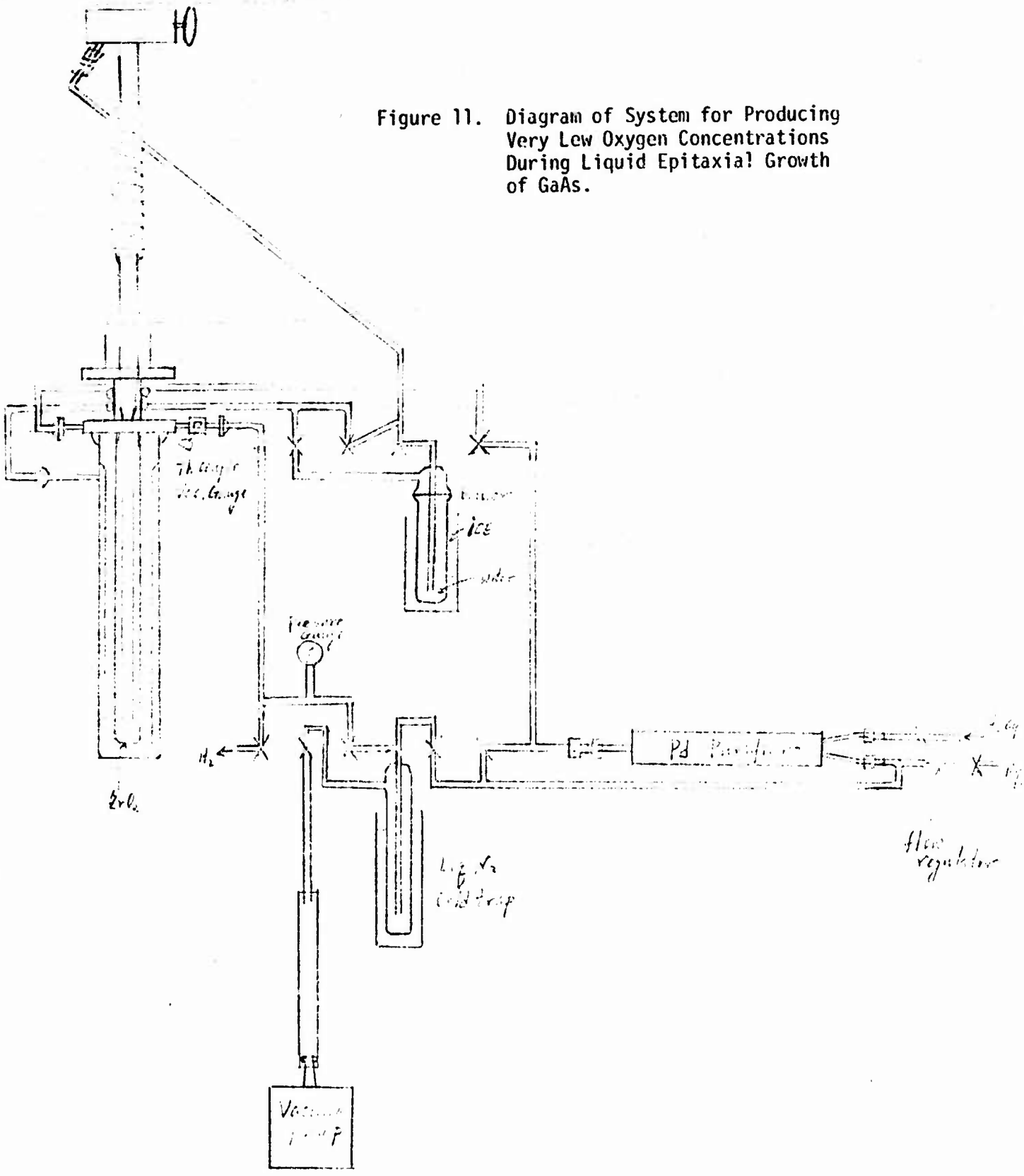

Figure 11. Diagram of System for Producing Very Low Oxygen Concentrations During Liquid Epitaxial Growth of GaAs.

defects are to be minimized. Such defects arise from local melting. Such local melting occurs at dislocations for (211) and (311) orientations. When this is prevented by providing a suitable partial pressure of As, these orientations can yield essentially defect-free films. We found that the insertion of GaAs chips in the inlet H_2 stream at the growth temperature to be a satisfactory method of introducing the As gas. This method minimizes problems with melt supersaturation and uncontrolled growth.

F. Related Crystal Growth Research

Solid foreign particles are known to generate new grains and twins when they are incorporated into a solidifying crystal. This has, for example, been observed during growth of GaAs by our new Czochralski technique. Thus we have a small project to investigate the influence of solidification conditions on particle incorporation using an organic analog. It has been found that particles are incorporated when the crystal growth rate exceeds a critical value. This critical freezing rate was found to increase substantially when the melt was stirred by rotation. The critical freezing rate and the dependence on stirring depended on the particle studied. This project should be completed by the termination of the grant period.

When GaAs is grown from solution or from non-stochiometric melts, Ga or As inclusions are sometimes formed in the crystal. Because of the dependence of solubility on temperature these inclusions should move in a temperature gradient imposed on the crystal during growth or later. We have briefly studied phenomena which occur when solvent inclusions are subjected to a temperature gradient [3]. Alkali halide crystals containing water and water-alcohol inclusions were used as convenient analog systems for study. It was confirmed that solvent inclusions move toward the heat source under ordinary conditions. As noted previously [4], the presence

of air bubbles caused the inclusions to move in the wrong direction. When the temperature was raised above the levels shown in Table I, boiling occurred in the inclusions (see Figure 12). This at first caused rapid movement, but then the travel rate fell to near zero. The solvent vapor

Table 1

Measured Boiling Points of Solvent Inclusions in Alkali Halide Crystals in a Temperature Gradient

Crystal	Solvent	Boiling Point
NaCl	water	321°C
NaCl	water-alcohol	296°C
KCl	water	249°C
KCl	water-alcohol	209°C
KI	water	137°C

pressures corresponding to these boiling points far exceed 1 atmosphere. Experimentally measured travel rates are summarized in Figures 13, 14 and 15. The dashed curves correspond to theoretical movement rates with water as a solvent, no air bubbles or boiling present, no convection in the inclusion, and infinite interface kinetics. We conclude from this data that there is an appreciable interfacial kinetics resistance to movement and that free convection was taking place in these ~0.5 mm diameter cylindrical inclusions, resulting in greater movement rates with a horizontal temperature gradient than with a vertical gradient.

A paper has been published on off-eutectic solidification, which would prove useful were oriented composites of, say, GaAs-As required [5]. A survey of motion pictures dealing with crystal growth has recently been completed [6].

Figure 12: Boiling in KI. Frame from motion picture.

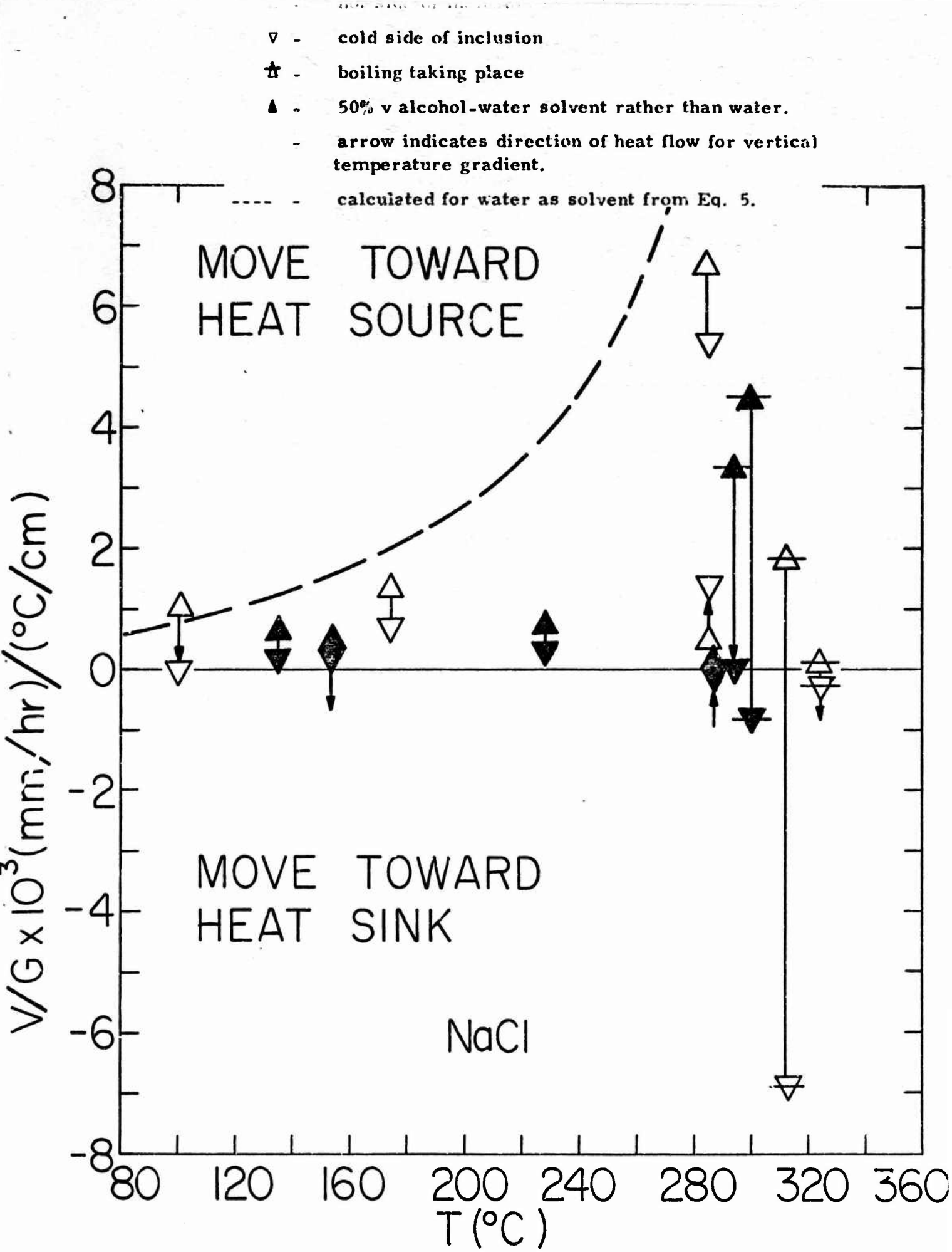

Figure 13 Rate of movement of solvent inclusions in NaCl/imposed temperature gradient. T is average temperature within inclusion.

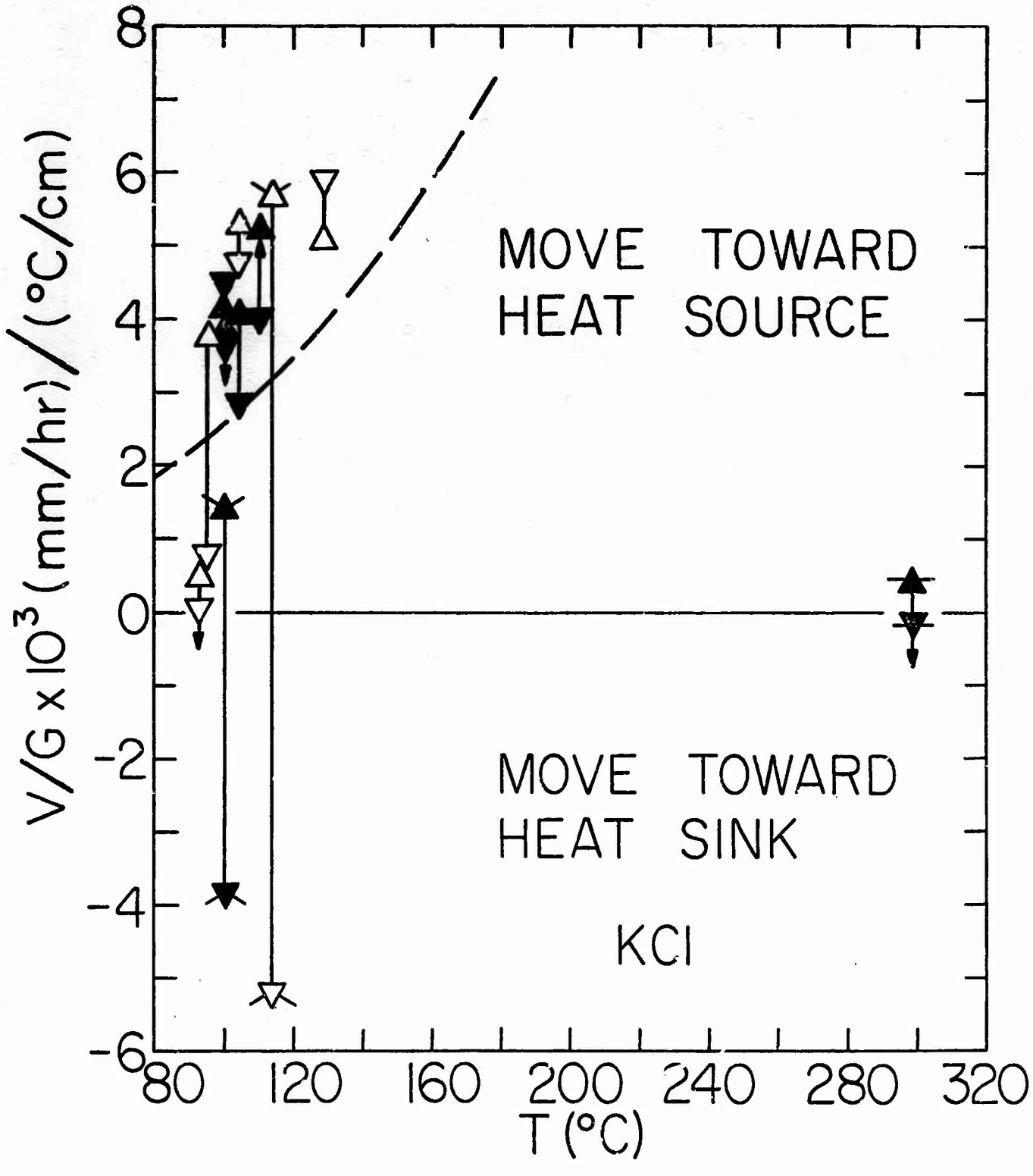

Figure 14 Rate of movement of solvent inclusions in KCl/imposed temperature gradient. Same notation as Fig. 1, plus following:

Y - air bubble present in inclusion.

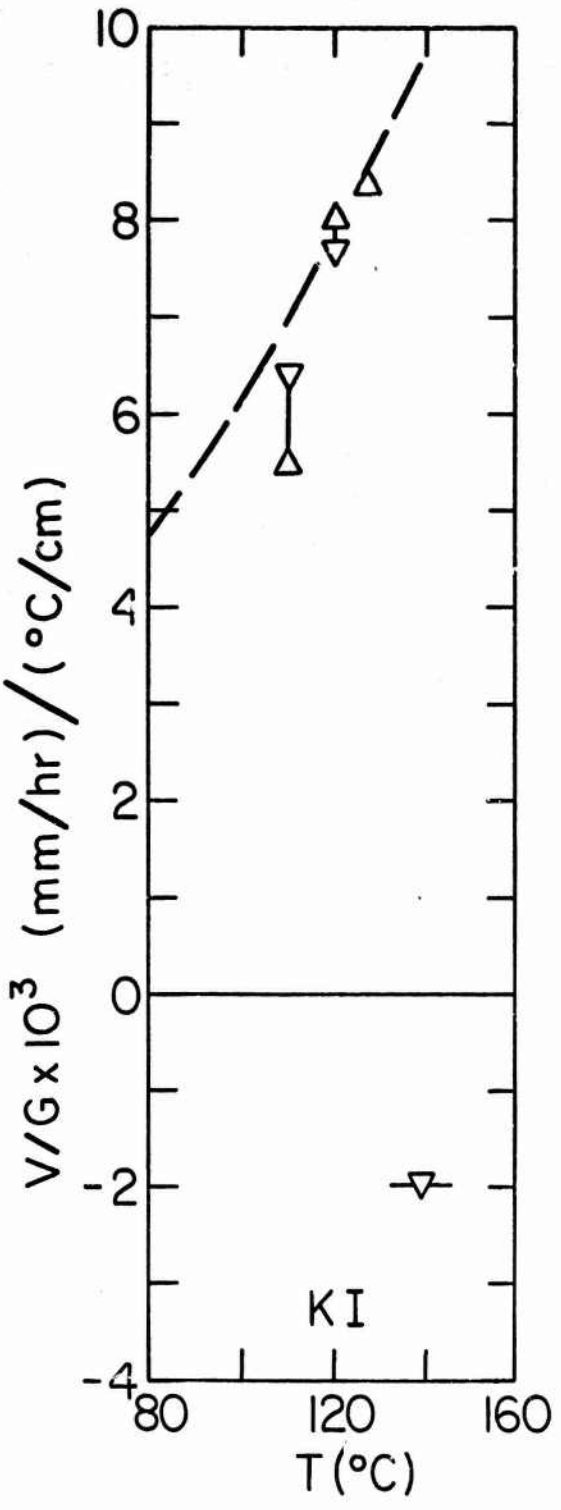

Figure 15 Rate of movement of aqueous inclusions in KI/imposed temperature gradient.

Same notation as Fig. 13

II. CHARACTERIZATION

A. Dislocation Studies and Electrical Properties

Our last report [1] characterized GaAs single crystals grown at USC by indicating the types of dislocations present on the polar surfaces of GaAs and the low density of grown-in dislocations present in crystals grown by the improved Czochralski method. The present report deals with dislocations introduced into the crystal in a controlled manner by plastic deformation. To study in detail the effects of dislocations on the electrical properties of compound semiconductors, dislocations of a specific type, such as edge dislocations, are produced by four-point bending (along a suitable bend axis) at elevated temperatures [7]. The method and apparatus used for this operation will be described. Electrical properties, chiefly Hall parameters, obtained from the as-grown, heated and bent crystals will be presented.

1. SAMPLE PREPARATION

GaAs samples chosen for the bending experiments were taken from a doped (Te: $10^{17}/cm^3$) Czochralski crystal (Ingot CZ-16) and an undoped crystal grown by the horizontal Bridgman method (Ingot HB-105). After suitably orienting the crystals by a standard X-Ray Laue technique, the samples were cut successively with a diamond wheel and a wire saw such that the bars could be bent along the $\langle \bar{1}\bar{1}2 \rangle$ direction (see inset, Figure 16).

The samples were 1.6 to 2.0 cm long, 0.12 to 0.17 cm wide and 0.10 to 0.15 cm thick. To remove any surface damage due to cutting, the rectangular bars were lapped on 3200 grit, etched in a nitric-hydrofluoric acid solution until about 50 microns were removed, and finally rinsed in

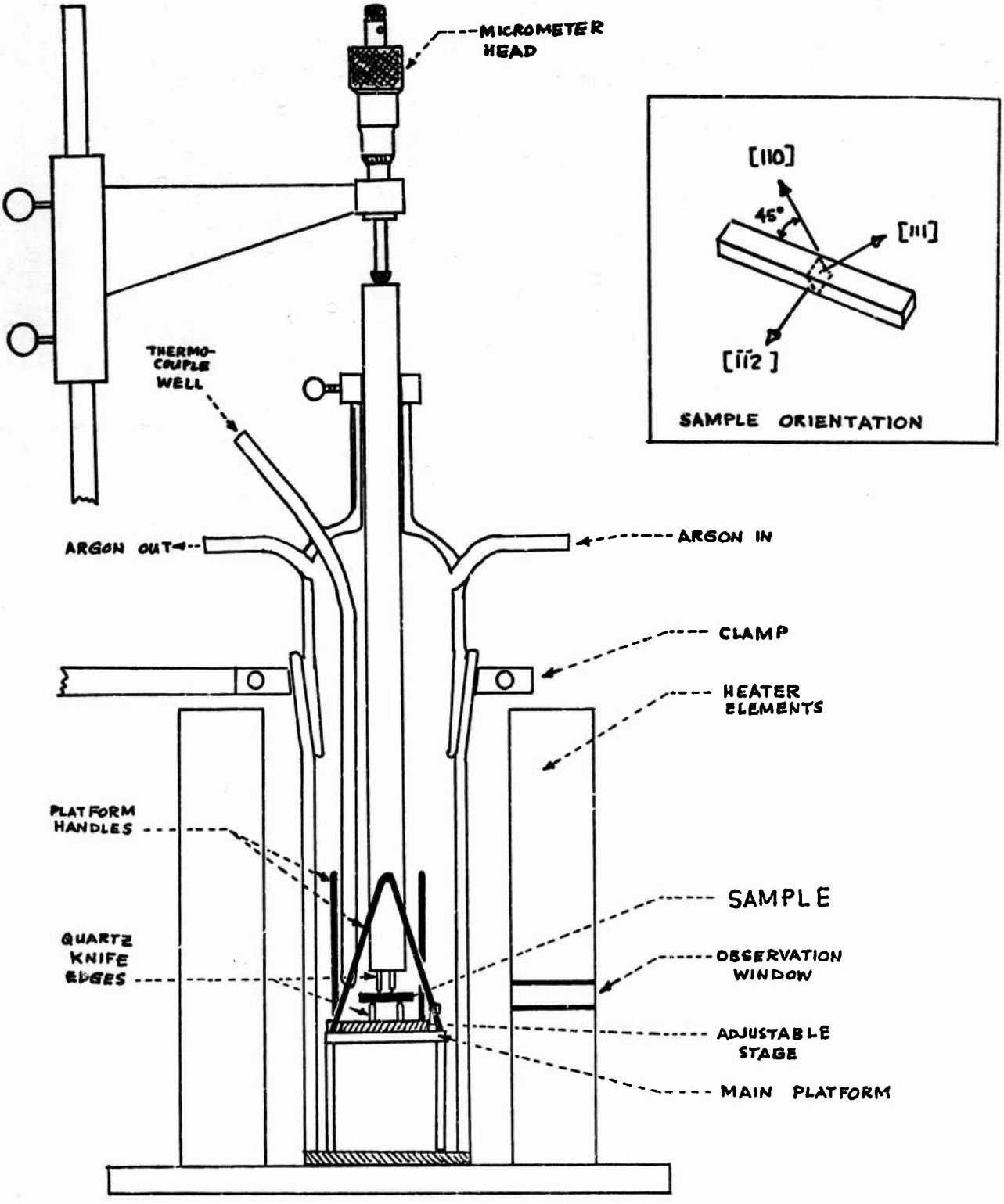

Figure 16. All-Quartz Bending Apparatus

deionized water. The resulting samples exhibited bright and shiny surfaces.

Six bar samples were cut from the same slice (no. 10) taken from approximately the center of CZ-16. The first two bars were used for control purposes (namely, as-grown and heated, not bent), and the remaining four were bent to various curvatures. Because the slices from the front end of the Bridgman crystal were slightly smaller than the Czochralski slices, only three bars (one for bending, the other two for control) could be cut from each slice. Thus, the four Bridgman samples were taken from four adjacent slices instead of from a single slice.

2. BENDING PROCEDURE AND RESULTS

The bending experiments were performed in an all-quartz apparatus (Figure 16) which was designed to eliminate sources of contamination likely to be present in a metallic or non-quartz system. The bending apparatus consists of a lower set of quartz knige edges with a separation distance of d_s = 1.24 cm mounted on a movable stage (to permit easier alignment) and an upper set of knife edges (d_s = 0.275 cm) attached to the tip of a 1.5 cm diameter quartz rod. The sample is set on the lower knife edges and kept in position by the upper knife edge. Bending is accomplished by turning the micrometer head a predetermined number of terms.

Prior to each bending operation, the quartz platforms were removed from the bottle by means of the arch-shaped handles (Figure 16) and washed with aqua regia, dilute HF, and rinsed in deionized water. To remove any residue from the cleaning, the entire bending apparatus was heated (minus the sample) to 700°C with two semi-cylindrical heating elements which surround the quartz bottle. Upon cooling, the platforms were again removed from the bottle and a sample positioned on top of the lower knife edges. For control purposes, another unbent sample was set beside the

lower knife edges on the movable stage. After flushing the quartz bottle for 15 minutes with purified argon, the furnace was heated to 700°C. Temperature was monitored by a previously calibrated chromel-alumel thermocouple which extended via a sealed quartz tube to the inside of the bottle down to the sample level (Figure 16).

The bending temperature range of 650 to 725°C was reached 15 minutes from the moment power was turned on. This heat-up time, however, will be reduced to 5 minutes with the use of a higher power variac. The actual bending of the sample took 30 seconds. Immediately after bending, which was observed and monitored through a port hole, power was turned off and the sampled cooled to room temperature by pulling the two heating elements away from the quartz bottle. Upon removal from the furnace, the bent and control samples were always found to retain their original shiny surfaces.

Using this bending procedure, the Czochralski and Bridgman grown GaAs samples were bent to various radii of curvature, R, which were measured graphically from enlarged photographs of the samples. The dislocation density, ρ, was calculated using Nye's relation [8], $\rho = 1/(Rb\cos\theta)$, where b is the magnitude of the slip vector, $\vec{b} = (a/2)\langle 110\rangle$, θ is the angle between the (111) slip planes and the neutral bend plane. The measured bend radii and calculated dislocation densities are listed in Table II and the dislocation density distribution of the samples is shown in Figure 17.

3. ELECTRICAL PROPERTIES

Five crystals grown by the Czochralski and Bridgman methods were studied. Two of the crystals were undoped, while the remaining three were doped with Te (10^{17} and 10^{18}) and Zn (10^{17}), thus providing both n- and p-type samples. The two crystals chosen for bending were taken from this batch of five crystals.

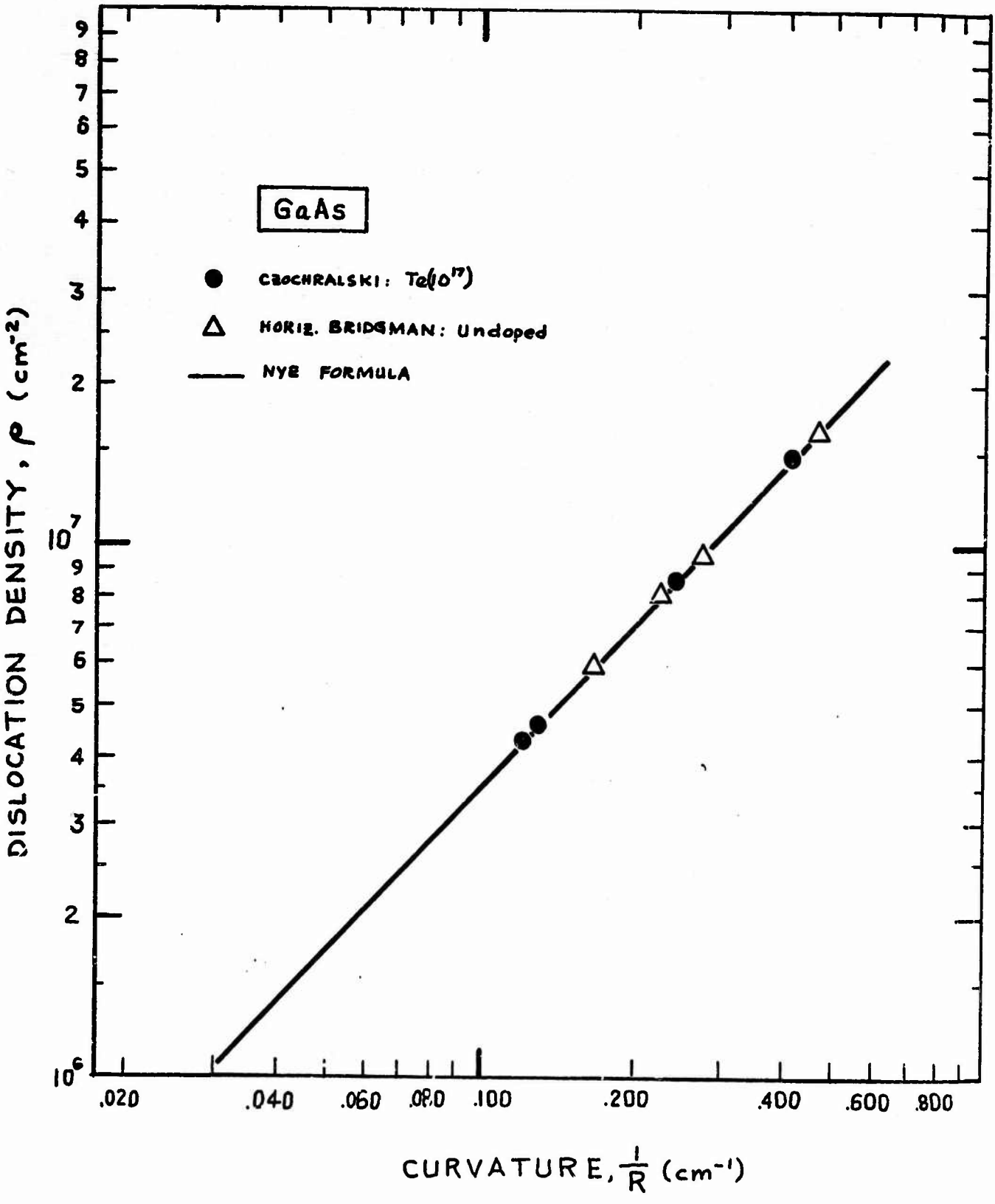

Figure 17. Dislocation Densities in Bent Czochralski and Horizontal Bridgman Crystals.

Table II.

Radii of Curvature and Dislocation Densities in Bent GaAs

Czochralski (Doped: Te $10^{17}/cm^3$) Sample No.	Radius of Curvature R (cm)	Curvature $\frac{1}{R}$ (cm^{-1})	Dislocation Density ρ (cm^{-2})
CZ-16: 10-F	8.30	0.121	4.28×10^6
10-E	7.62	0.131	4.64×10^6
10-C	4.13	0.242	8.57×10^6
10-D	2.42	0.414	1.47×10^7

Horizontal Bridgman (undoped) Sample No.	R (cm)	$\frac{1}{R}$ (cm^{-1})	ρ (cm^{-2})
HB-105: F13-C	4.98	0.167	5.91×10^6
F11-C	4.44	0.225	7.97×10^6
F12-C	3.78	0.265	9.38×10^6
F10-C	2.13	0.469	1.66×10^7

Hall parameters were calculated from resistivity and Hall voltage data obtained at room and liquid nitrogen temperatures from a DC Hall apparatus with a 5 kG magnet (U.S. Naval Electronics Laboratory, San Diego, California). Sample currents varied from 10 to 20 mA. Reproducibility of the measurements was 1 to 2% for the resistivity data and 2 to 5% for the Hall coefficient, mobility and carrier concentration.

Because of the bar shape of the samples, some difficulty was encountered in appropriately installing ohmic contacts. Three methods were evaluated. The first method consisted of simply soldering indium at six points of the bar corresponding to the six arms in a Hall bridge sample. The contacts were non-ohmic, displaying non-linear and asymmetrical voltage-current characteristics, and yielded a sample resistance of 4000 ohms or greater. The second method was the evaporation of a Au-Ge eutectic alloy onto the current contacts of the sample after the method of Clawson and Wieder [9]. To keep the Au-Ge film from curling up during the alloying process, a layer of indium oxide was evaporated on the Au-Ge film. Alloying of the Au-Ge with the GaAs surface was accomplished by exposing the sample to a 400°C heat lamp. The indium oxide was subsequently removed by gently abrading the contacts. The resulting contacts were ohmic and yielded a resistance of 0.4 ohm.

The third method consisted of soldering a small amount of indium at the desired locations on the bar sample and applying momentarily the edge (not the tip) of an oxy-hydrogen flame to the spots of indium. This method assured proper alloying of the indium with the GaAs surface and yielded linear and symmetrical voltage-current curves with a sample resistance of 0.1 to 0.2 ohms.

The effect of heating during the flame soldering process was evaluated

by comparing the Hall measurements taken from the same sample to which the two types of contacts were successively bonded. The first set of Hall measurements were taken after Au-Ge was evaporated onto the top surface of the bar ends (current contacts), while the second Hall data were measured after indium was flame soldered to the edge surfaces of the bar ends. Comparison of the Hall parameters taken at room and liquid nitrogen temperatures indicated a difference between the two methods of 2 to 3% in the resistivity data, and a difference of 5 to 8% in the Hall coefficient, mobility and carrier concentration. A similar range of percent differences was found between Hall measurements taken from the same sample after a first and then a second exposure to flame soldering.

This third method of attaching indium contacts by flame soldering was subsequently adopted because it yielded low resistance ohmic contacts and because the percent differences in the measurements were within the experimental error. A further reason for using this method was that with the aid of a suitably designed sample holder, the leads could be attached to the sample with a minimum of sample handling and with no subsequent cleaning.

3. RESULTS AND DISCUSSION

The results of Hall measurements taken from the five crystals are summarized in Figure 18. These data indicate little variation with temperature (at 77 and 300°K) of the conductivity, mobility and carrier concentration in the crystals with relatively high carrier concentrations (10^{17} cm^{-3} or greater). Although only two temperature points are shown in Figures 18 and 19, preliminary results from Hall measurements taken at temperatures ranging from 80 to 300°K (in steps of 10 to 15°K) indicate almost linear curves with negligible slopes. A trend of decreasing mobility with

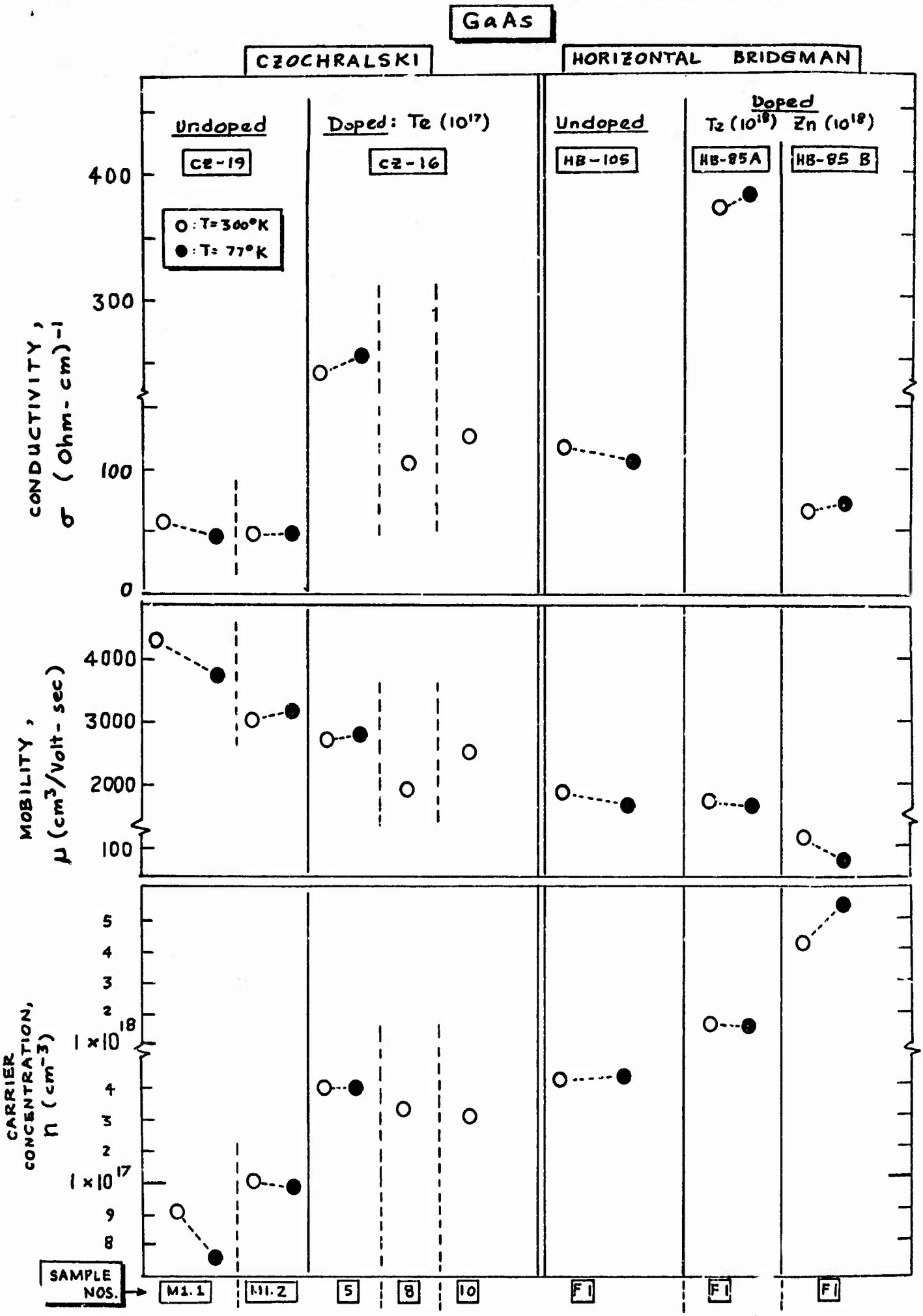

Figure 18 Variation of Hall Parameters in Five As-Grown

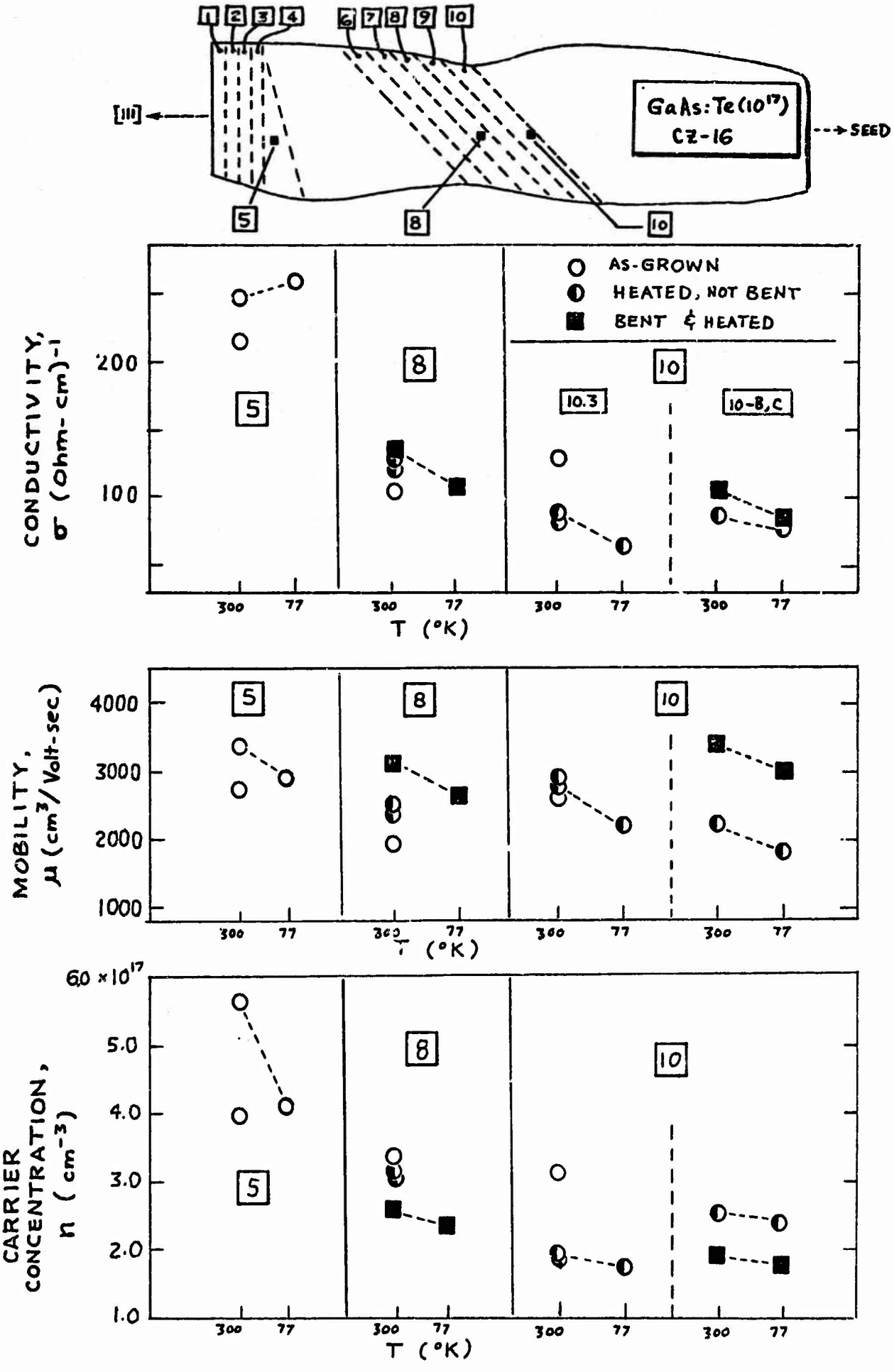

Figure 19. Hall Parameters Before and After Bending of Samples Taken from Different Sections of a Czochralski Grown GaAs Crystal.

increasing carrier concentration is evident for the five crystals (Figure 18) although no systematic increase was noted for the conductivity.

To test the variation of the electrical properties of the as-grown Czochralski crystal with distance along the length of the crystal, samples were selected from three portions of the crystal (shown schematically in Figure 19). The results of Hall measurements taken at room and liquid nitrogen temperatures before and after heating and bending are shown in Figure 19.

Figure 19 shows the increase in conductivity and carrier concentration with increasing distance away from the seed end of the crystal (slices 10 and 8 to 5). The sample from slice 5 exhibits a marked variation of carrier concentration with temperature as well as a relatively higher conductivity than slices 8 and 10. In contrast to the region of slice 5, the central portion occupied by slices 8 and 10 appears to possess a more uniform set of electrical properties.

Heating the control samples taken from slices 8 and 10 to 700°C reduced (relative to the as-grown properties) the carrier concentration, and increased the mobility. However, opposite effects due to heating were noted in the conductivity of No. 8 (which increased) and of No. 10.3 (which decreased) after heating, an effect accompanied by a drop in carrier concentration.

The effects due to bending (relative to the heated, unbent samples) in samples 8 and 10-C follow a more consistent trend in that a decrease in carrier concentration was accompanied by an increase in mobility and a slight increase in conductivity. While the decrease in carrier concentration after bending is frequently attributed to precipitation of impurities in the dislocations generated by the bending, it is not clear why heating the control, unbent sample (10.3) caused a drop in the carrier concentration

larger than that observed between the heated and bent samples (10-B,C). These results are still being evaluated and final interpretation will be made upon completion of Hall measurements currently being undertaken on a cooperative basis (through courtesy of Dr. H. Wieder) at the Naval Electronics Lab Center, San Diego, California.

4. SUMMARY AND FUTURE WORK

Present Hall measurements indicate definite measurable effects on the Hall parameters due to plastic deformation by bending. The effect of the short term heating of the control sample is not clearly understood and will be investigated further. Also, it is known that α and β dislocations in A^{III}-B^{V} compounds produce opposite effects on the Hall coefficient [10]. This phenomenon can be studied in GaAs by simultaneously bending two oppositely oriented bar samples. Hall measurements are currently being conducted to show a more detailed variation of the Hall parameters with impurity concentration, temperature, and dislocation density. Dislocation etch pit studies employing optical microscopy will also be made of the bent samples.

B. Cathodoluminescence and Stimulated Emission Studies

Since the last report [1] equipment difficulties have been encountered with the cathodoluminescence investigation of GaAs, GaP and $GaAs_xP_{1-x}$ semiconductors. The electron microprobe which is being used to analyze the $GaAs_xP_{1-x}$ samples and to do room temperature cathodoluminescence studies has had high voltage power supply problems, vacuum leaks, vacuum pump failure and X-ray spectrometer failure. As of now, all the above problems have been corrected. A new oil diffusion pump has been installed which provides 30% greater pumping speed. This, along with correcting

leaks in the probe tank, has improved the vacuum to better levels than achieved in the past year.

Some measurements of X-ray intensities have been made on $GaAs_xP_{1-x}$ alloys. However, since the X-ray spectrometer cable failed during these measurements, they are now being repeated. When the X-ray measurements are completed, further cathodoluminescence spectra will be taken at low temperatures (~30°K) using the clean vacuum electron beam column. This system is described in detail in a recently published paper [11].

Stimulated emission studies have also been restricted due to the equipment problems described above. Nevertheless, the spectral distribution of radiation from GaAs has been studied as a function of electron beam current density at room temperature and at 113°K. Surprisingly, the results reported by Casey and Kaiser [12] (at room temperature) could not be duplicated even at 113°K with specimens taken from an adjacent wafer of the same ingot of GaAs. Further investigations are being made to determine the effects of surface treatment, sample geometry, and possibly sample mounting techniques. Curves of beam current versus peak radiation intensity and beam current versus radiation energy peak show a linear decrease of peak energy with beam current at both room temperature and at 113°K. At 113°K the rate of decrease of the peak energy increases after the beam current reaches a certain value. While Casey and Kaiser did not observe this linear shift of energy peak with current, our observations could be attributed to improper thermal contact between sample and sample holder which causes a large temperature rise of the sample during electron irradiation.

A decrease of radiation intensity with beam current after a certain value of beam current is reached has also been observed. At 113°K this

effect occurred at higher beam current than at room temperature. This intensity decrease could also be attributed to heating of the sample by the electron beam. Further studies will be made on more carefully mounted samples to eliminate this sample heating.

C. High Impedance Hall Apparatus

As reported in Section II.A, we have made a host of Hall measurements at the computerized facility at the Naval Electronics Laboratory, San Diego. For occasional measurements, a manual Hall effect apparatus has been constructed at USC for moderate resistivities. Measurements can be made from 4.2 to 300°K. A more sophisticated system for high resistivity samples has been constructed and is undergoing final testing and modification. The current source for the Hall samples is programmable and designed to eliminate effects of cable capacitance and cable leakage. The current source has an effective leakage resistance greater than 10^{12} ohms. A balanced varactor bridge differential voltmeter is used to measure the Hall voltage. This voltmeter features electronic suppression of the effects of cable capacitance and an electronically-driven common for the voltage circuit. This should provide a common mode suppression of leakage effects equivalent to leakage resistances on the order of 10^{12} ohms, a feature which is presently being tested. The system should be capable of making meaningful measurements on samples with resistances of $\sim 10^{10}$ ohms. It can also be used for AC Hall effect measurements with excellent noise rejection when combined with an additional phase sensitive detector.

D. Tunnel and Thermal Effects in Photoemission from Schottky Barriers

The theoretical work reported previously [1] has been extended to include effects of conservation of transverse momentum as a carrier crosses

a metal-semiconductor interface. We have also carried out further optimization of the computer program for tunneling probabilities. A paper has been prepared on "A Simple Precise Equivalent to the Fowler Photothreshold Plot." This treatment covers only the thermal tail in photoemission, but is a completely general treatment of this subject. The evaluation of thermal and tunneling effects requires a specific calculation for each semiconductor and temperature. Results for Si and GaAs are nearly complete and will be submitted for publication during the next six months.

E. Schottky Barrier-Capacitance Characterization of Impurities

Our capabilities for capacitance-voltage and conductance-voltage measurements on Schottky barriers are presently: bridge measurements from 20 Hz to 500 kHz and 1 mHz; direct reading electronic measurements using an operational amplifier system and phase sensitive detector from 2 Hz to 200 kHz. We have redesigned the front end of this system and are in the process of substituting an externally damped bridged T feedback system for an underdamped system which showed poor ability to balance in the presence of transients. This system uses small ($\sim$10 mV) modulation voltages from very low impedance sources and an operational amplifier sensing point at virtual ground which eliminates stray effects of cables and permits measurement of unknowns in remote locations, such as cryostats. Circuitry for frequency scanning and impurity profiling using the revised front end are being debugged. The impurity profiler system has a tolerance for and rejection of conductance effects which exceeds any reported system.

A limited number of point-by-point measurements on Pt-n-type GaAs Schottky barriers have been made to debug sample fabrication techniques for C-V measurement. Figure 20 shows $1/C^2$ versus V results for a nominal

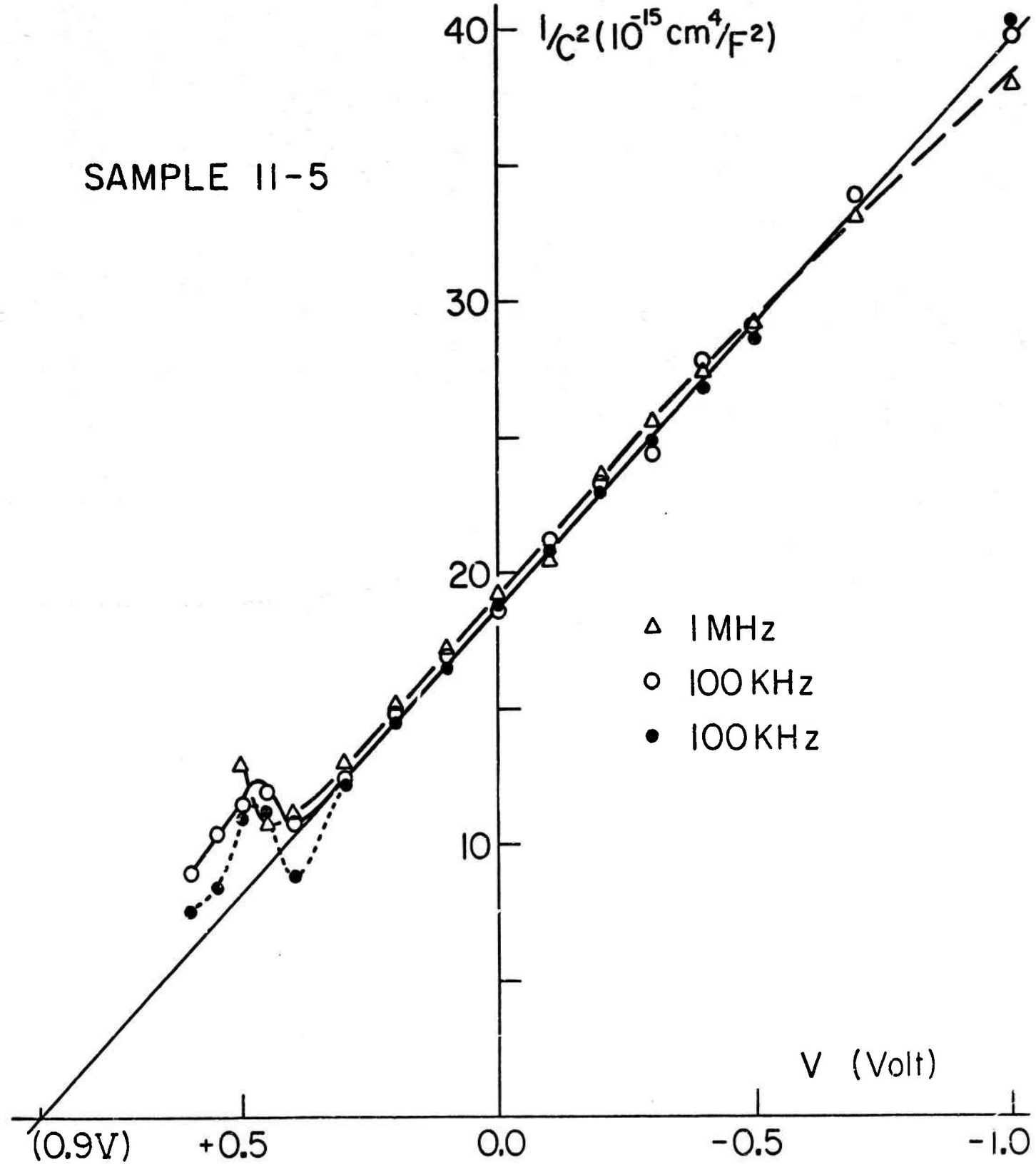

Figure 20. Capacitance-Voltage Measurements on Pt-n-type GaAs Schottky Barrier.

Te doping of 1.6×10^{16} cm^{-3} (300°C Hall measurement). The results on chemical-mechanical polished and solvent-rinsed surfaces showed large anomalies, presumably due to damage of the surface layer in polishing. Chemically etched samples, on the other hand, had much straighter $1/C^2$ versus V relationships at large reverse bias (indicating homogeneous doping of 4×10^{16} cm^{-3}), but had an anomaly starting at ~0.5 volts forward bias. This anomaly was not observed with a sample from another crystal of comparable doping. The cause of this anomaly is under active investigation.

With completion of the scanning capacitance system, routine acquisition of similar capacitance and conductance data and Hall effect measurements is planned for all newly prepared GaAs. Theoretically derived methods for interpreting the above measurements, especially capacitance-frequency measurements, are still under active development. We have succeeded in developing a simple multiple-branch R-C equivalent circuit which we feel will yield order of magnitude values for energy levels and capture cross-sections of the predominant deep-level traps in GaAs and mixed III-V crystals.

F. GaAs Photoluminescence Measurements

Low-temperature photoluminescence measurements have been made on GaAs samples cut from six crystals grown at USC. Five of the samples were grown by the liquid-sealed Czochralski technique (Section I.A), the sixth was grown by the horizontal Bridgman technique. One of the Czochralski-grown crystals and the Bridgman-grown crystal were not intentionally doped, the remaining crystals were doped with Te and combinations of Mg, S and Se. Photoexcitation was by helium-neon laser (6328 Å, 1.96 eV), filtered to remove long-wavelength laser lines. Photoemission in the wavelength region 0.8 to 1.05μ (1.55 to 1.18 eV) was analyzed with a

Perkin Elmer E1 monochromator and detected with a cooled RCA 7102 photomultiplier. The photomultiplier output was amplified by conventional phase-sensitive techniques and recorded on chartpaper.

Luminescence measurements in GaAs are complicated by the fact that impurity banding occurs at very low impurity concentrations ($\sim 10^{16}/cm^3$) due to the low carrier effective masses. Such banding greatly broadens the energy levels associated with impurity-assisted recombination. Thus, when banding occurs it is often possible to determine the general class of impurity present (shallow donors, deep acceptors, etc.) and the transition mechanism involved, but it is not possible to identify impurity atomic species.

Of the samples examined, only the Bridgman-grown speciman was pure enough to show some luminescence from free excitons or from excitons bound to neutral shallow donors or acceptors. Even in this sample, the dominant luminescence appeared to involve free-to-bound or shallow donor-acceptor pair recombination. The undoped Czochralski-grown sample appeared to be less pure and gave evidence of possible donor-acceptor pair or free-to-bound acceptor recombination. This result is in general agreement with the results of other characterization studies of this material which suggest compensation and Si contamination. The spectra from the Te-doped GaAs were dominated by possible free-to-bound transitions involving the Te donor. Some evidence for bound exciton recombination at neutral Te donors exists in the more lightly doped sample. In the more heavily doped sample, contamination by deep acceptor impurities such as Fe, Zn, Cd, Cu, etc., is suggested. The Mg:Se- and Mg:S-doped samples produced broad-band luminescence which could be interpreted as donor-acceptor pair recombination. Other interpretations involve Si or some deep acceptor. More exact interpretation of the data simply is not possible due to the effects of impurity

banding and the confused and often contradictory state of the GaAs photoluminescence literature. It should be pointed out that free and bound exciton recombination are not commonly observed in bulk GaAs and that nearly all such spectra reported come from high-purity epitaxially-grown material.

REFERENCES

1. Final Technical Report, "New Methods for Growth and Characterization of GaAs and Mixed III-V Semiconductor Crystals," ARPA Order No. 1628, Grant No. DAHC15-70-G14 (July 1971).

*2. C. E. Chang and W. R. Wilcox, Mat. Res. Bull. 6, 1297 (1971)

*3. K. Chen and W. R. Wilcox, submitted for publication.

4. W. R. Wilcox, Ind. Eng. Chem. 61, 76 (March 1969).

*5. R. T. Pepper and W. R. Wilcox, J. Composite Materials 5, 465 (1971).

*6. W. R. Wilcox and P. J. Shlichta, J. Crystal Growth (in press).

7. J. D. Venables and R. M. Broudy, J. Appl. Phys. 29, 1025 (1958).

8. J. F. Nye, Acta Met. 1, 153 (1953).

9. A. Clawson and H. Wieder, U.S. Patent No. 3,532,562 (6 Oct. 1970).

10. R. L. Bell and A. F. W. Willoughby, J. Mat. Sci. 5, 198 (1970).

*11. H. C. Marciniak and D. B. Wittry, Rev. Sci. Instr. (Dec. 1971).

12. H. C. Casey, Jr., and R. H. Kaiser, Appl. Phys. Letters 8, 113 (1966).

*13. C. Crowell, et al., submitted for publication.

---

*Papers acknowledging ARPA support.